J. Exp. Mar. Biol. Ecol., 150 (1991) 163–182

JEMBE 01620

Deep-water rhodolith distribution, productivity, and growth history at sites of formation and subsequent degradation

Mark M. Littler[1], Diane S. Littler[1] and M. Dennis Hanisak[2]

[1]*Department of Botany, National Museum of Natural History, Smithsonian Institution, Washington, District of Columbia, USA;* [2]*Marine Botany Department, Harbor Branch Oceanographic Institution, Fort Pierce, Florida, USA*

(Received 29 May 1990; revision received 5 March 1991; accepted 20 March 1991)

Abstract: This study provides the first quantitative measures of deep-water (i.e., below scuba depths) rhodolith development, distribution, abundance, and primary productivity at sites of both active formation and breakdown. The 1.27-km^2 upper platform surface of San Salvador Seamount, Bahamas, ranges in depth from 67 to 91 m and averages 95.8% cover of rhodoliths that contribute an estimated 391 t organic C · yr^{-1} to deep-sea productivity. The predominant nongeniculate coralline alga of the slope environment has an extremely narrow *PI* curve (photosynthesis vs. irradiance) of net primary production (0.005 to slightly beyond 0.24 μmol · m^{-2} · s^{-1} PAR) suggesting that some deep-water benthic algae may be acclimated to restricted light ranges. Platform areas contain up to five-deep accumulations ($\approx$45 cm thick) of rhodoliths with their visible, planar (2-D), crustose algal cover (68.5%) composed of 41% *Lithophyllum* sp., 14.9% other nongeniculate corallines, and 12.6% *Peyssonnelia* sp. Platform rhodoliths also contain $\approx$25% average planar cover of the foraminiferan *Gypsina* sp. overlying the rock-penetrating chlorophyte *Ostreobium* sp.

On the steep slopes of the seamount, to a depth of 290 m, rhodoliths that have spilled down from the relatively flat platform average 17.4% cover. These nodules tend to be concentrated in fan-shaped deposits that are most prevalent (33.3% cover) on the west side (leeward) of the mount where they are more abundant near the top of the slope than on the other three sides. Cover of living crustose algae on the deeper slope rhodoliths averages only 22.8% and is made up of 14.8% unidentified nongeniculate corallines, 6% *Lithophyllum* sp., and 2% *Peyssonnelia*. *Gypsina* sp. is not an important component of the slope nodules. Biotic overstory on the seamount slopes is greatly reduced relative to the platform, restricted mainly to bedrock, and consists mostly of *Halimeda*, gorgonians, and sponges along with scattered patches of small frondose algae.

Over platform depths from 67 to 91 m, rhodoliths are fairly uniform in composition and abundance. Ranging from 4 to 15 cm in diameter, with an average of $\approx$9 cm, they are roughly spherical with smooth living surfaces. The rhodoliths spilling down the steep slopes of the seamount to depths below 200 m are characteristically smaller (mean of $\approx$5 cm diameter), much rougher, and pitted by boring organisms. As shown by cross sections through the centers of the platform nodules, outer, relatively thin (1–3 cm thick), well-preserved envelopes overlie dead laminated crustose layers. These layers surround much thicker cores of biotically altered carbonate (mostly coralline, foraminiferan, and coral) that have been extensively reworked by boring sponges, algae, polychaetes, and pelecypods. Borings have been infilled with carbonate detritus and are lithified to various degrees ranging from porous to dense and stony.

Radiocarbon dates indicate that the outermost unaltered envelopes that underlie actively growing crusts are 112–880 yr old ($\bar{x}$ = 429 ybp), while the innermost unaltered layers average 731 ybp (range = 200–1100 ybp). The consistently abrupt transitions from the intact underlying layers of living

Correspondence address: M.M. Littler, Department of Botany, National Museum of Natural History, Smithsonian Institution, Washington, DC 20560, USA.

Contribution 245 of the Smithsonian Marine Station at Link Port, Florida, and Contribution 814 of the Harbor Branch Oceanographic Institution.

rhodoliths to the older reworked cores ($\bar{x}$ = 1023 ybp, range = 625–1295 ybp) corroborates the major discontinuities in growth found by other workers. It appears that most rhodoliths are likely to become buried for substantial periods in their long histories during which time bioerosive forces exceed accretion, which will be recorded as discontinuities in the growth patterns following re-emergence.

Key words: Coralline alga; Deep water; Productivity; Rhodolith; Seamount

INTRODUCTION

Descriptions of spheroidal carbonate nodules dominated by populations of nongeniculate coralline Rhodophyta (rhodoliths, coralline algal nodules, algaliths, or rhodolites) date to the observations of Weber-van Bosse & Foslie (1904) who noted rhodoliths "as far as the eye can see" on the intertidal reef flat at Haingsisi, southwestern Timor. The geological and biological importance of these structures was noted first by Bosellini & Ginsburg (1971). Further research on rhodoliths has been reviewed by Bosence (1983).

Although this study is restricted to depths where only encrusting nongeniculate (formerly termed "crustose") coralline algae occur, Hay (1986) provides convincing theory on thallus form–light energy relationships that may explain the decrease in abundance from branched to columnar to encrusting forms as a function of increasing depth. Littler et al. (1986) noted four major zonal assemblages, dominated by *Lobophora*, *Halimeda*, *Peyssonnelia*, or an unidentified nongeniculate coralline alga, as a function of depth on the bedrock substratum of San Salvador Seamount, Bahamas. Distributional records for attached frondose and encrusting algae, as well as the light attenuation curve for San Salvador Seamount (see Littler et al., 1986) indicate a light regime that never exceeds 0.0015–0.027 μmol $\cdot$ m^{-2} $\cdot$ s^{-1} (PAR) at the extinction depth (268 m) of the deepest-growing nongeniculate coralline alga. The observation of active growth, indicated by abundant new thallus cell divisions, suggested (Littler et al., 1986) evolutionary adaptation to this extreme light environment, equivalent to a light attenuation of 0.00005–0.0009% of the maximum surface irradiance.

Several workers have emphasized the utility of rhodolith morphology and age as paleoenvironmental indicators (e.g., Logan et al., 1969; Bosellini & Ginsburg, 1971; Toomey, 1975; Focke & Gebelein, 1978; Bosence, 1983; Scoffin et al., 1985; Prager & Ginsburg, 1989). For example, abrupt transitions in age have been noted (400 $\pm$ 40 yr before present, McMaster & Conover, 1966; 645 $\pm$ 45 ybp, Focke & Gebelein, 1978; 330–550 ybp, Reid & Macintyre, 1988) from the intact outer underlying layers of living rhodoliths to the older bored and infilled cores, indicating major discontinuities in growth. The broad similarities in previously reported structures and radiocarbon dates of nodules from diverse regions such as Campeche Bank, Flower Garden Banks, Bermuda Platform, Canary Islands, and throughout the eastern Caribbean Islands have been interpreted by the detailed and careful study of Reid and Macintyre (1988) to indicate comparable geological histories. For example, accretion occurred at $\approx$0.04 mm $\cdot$ yr^{-1} for an average of $\approx$500 yr following the suggestion of a widespread

paradoxical hiatus (see Reid & Macintyre, 1988) during which growth ceased and nodules were bored, infilled, and lithified.

Traditionally, deep-water rhodolith studies have been restricted to dredging (Barnes et al., 1971; Weydert, 1974; Faure & Montaggioni, 1976; Focke & Gebelein, 1978; Minoura & Nakamori, 1982; Reid & Macintyre, 1988; Prager & Ginsburg, 1989), a method yielding a minimum of ecological information and unsuited for characterizing small-scale environmental conditions. A comprehensive study utilizing submersibles and in situ techniques (Earle, 1985), by providing the first quantitative survey of abundance patterns and primary productivity below scuba depths, has the potential to clarify uncertainties concerning the formation of rhodoliths and their role in the deep sea. In this paper we analyse the distribution, composition, photosynthetic, and growth patterns of rhodoliths at the sites of active formation on a seamount platform near San Salvador Island, Bahamas, and follow their transition to deep-water slope environments where bioerosional forces predominate and growth becomes inactive.

Methods and Materials

STUDY AREA

San Salvador Island, located along the eastern margin of the Bahamas (Fig. 1, 24°02′N, 74°30′W), is ≈612 km east-southeast of Miami, Florida, and 346 km north of Cuba. We became intrigued by an uncharted region off the northern tip of the island where gradual slopes having extensive algal nodules were noted in earlier studies (Littler et al., 1985, 1986). Fathometer tracings of the area (see Fig. 1, inset) revealed a seamount (herein referred to as San Salvador Seamount, SSSM) 6.5 km north of San Salvador Island (Fig. 1, 24°13.7′N, 74°29.0′W). An isobath tracing at 91 m showed a 1.27-km^2, nearly horizontal platform (67–91 m depth range, north to south) above the steeply rounded margin. The surrounding slopes average ≈28% on the south side, 57% on the west and north sides, and are nearly vertical on the upper eastern portion, descending to depths in excess of 830 m. The topographic isolation of the seamount from the island by waters to 360 m deep presented a unique sedimentary-source ecosystem where in situ nodule formation could be studied with extrinsic import not a factor.

NODULE STANDING STOCKS

During 27–29 October 1985, the substrata and biota on the east, west, north, and south slopes of SSSM were videotaped at right angles in continuous belt transects beginning at a depth of 520 m and continuing slowly upward across the top to the center of the seamount platform on fixed compass headings. A Marine Optical Systems 3000 videocamera and Benthos 372 35-mm camera, mounted externally on the frame of the *JOHNSON-SEA-LINK I* submersible, recorded the imagery at right angles to the

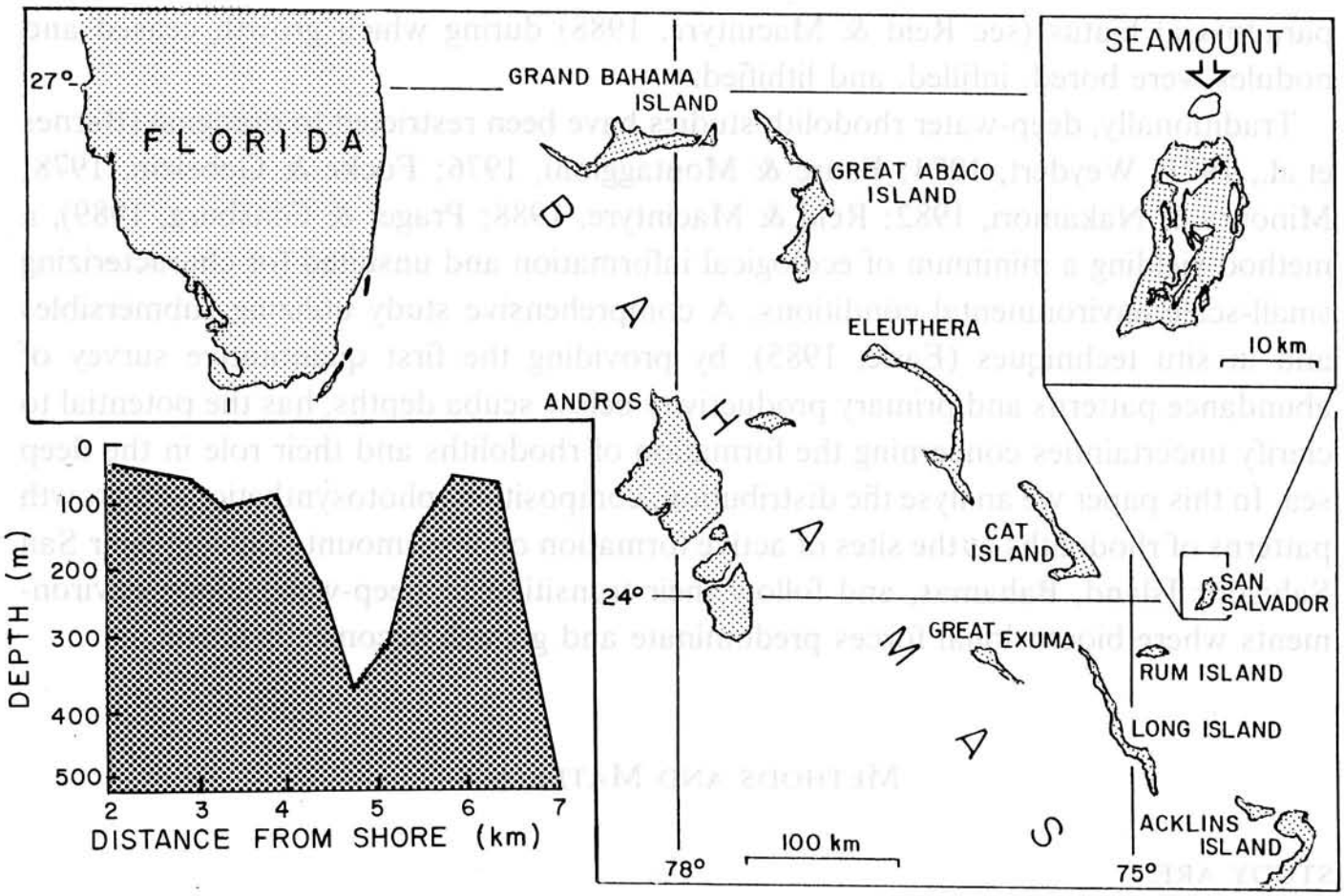

Fig. 1. Location of San Salvador Island Seamount and profile made from south to north fathometer tracings (inset).

substratum. A 1-m Al rod calibrated at 10-cm intervals was mounted externally where it could be positioned in slight contact with the substratum, providing a sample scale and right-angle orientation when framed at the upper margin of the videomonitor. This rod pushed frondose and other upright organisms aside revealing the understory nodules. Concurrent detailed field notes and collections were made of the dominant organisms and nodules. Visual in situ estimates of planar (2-D) nodule cover and of biotic coverages on the nodules were made from 290 m upward (range of living nodules) and updated continuously on a taperecorder. Because light energy is thought to be a critical factor for deepwater algae (Hay, 1986) and photosynthesis of crustose algae correlates most closely with 2-D area normal to the incoming radiation (Littler, 1973), we chose to measure planar area rather than the relatively intractable 3-D area of living rhodolith cover. On the platform, coverages of dense overstory canopies of frondose algae were estimated and moved aside by the calibrated rod to permit videoscoring of understory and encrusting layers.

The submersible also was equipped with a temperature probe, conductivity meter, and Li-Cor LI-550 printing integrator with a 192s cosine response light sensor, which recorded data that were referenced to the transect estimates at specific depth intervals. Data from these readings indicated a relatively constant environment since they did not differ substantially from those taken during earlier observations in mid-October 1983

(see Fig. 2 of Littler et al., 1986), e.g., the photon flux density was characteristic of the clearest of oceanic waters (Type I, Jerlov, 1970) while temperature and conductivity decreased at constant rates with slightly more abrupt declines near the platform.

In the laboratory, four square quadrats, each 60 × 60 cm (0.36 m^2), were selected by randomly determined tape distances from each 14–15-m depth interval throughout the depth range 67–290 m recorded by the continuous belt-transect videotapes. The resultant 317 quadrats were each projected on a Sony high-resolution videomonitor and "scored" in stop action at the predetermined intervals to gain accurate documentation concerning the distribution and planar cover of the nodules and their living biota. Scoring was accomplished by stratified random dots on two 27 × 35-cm transparent vinyl sheets. Every stop-action videotape quadrat was scored twice with the two different grid arrays ($\approx$70 dots each) that were each positioned without regard to the fields of view to assure unbiased replication. Encrusting species were scored for those portions of the quadrats where upper canopies were moved aside. A total of $\approx$ 140 point intercepts, randomly distributed within adjacent 2 × 2-cm squares on the vinyl sheets, were scored per quadrat. This technique has been shown (Littler & Littler, 1985) to provide an appropriate density for consistently reproducible estimates of cover. The percent cover values were expressed as the number of "hits" for all substratum types and species, divided by the total number of dots contained within the quadrats for each replicate scoring. Reproducibility was consistently high when this technique was repeated for the same quadrat and seldom varied $> \pm 5\%$ for the dominant taxa. We analysed differences between total rhodolith cover (following arcsine transformation) on the platform vs. slopes, and between the east vs. west vs. north vs. south platform and slope transects independently, by one-way ANOVA (Sokal & Rohlf, 1969). The Bonferroni a posteriori multiple classification analysis (SAS, 1985) was used to identify significant groupings. Similar statistical comparisons were made for total cover of living encrusting algae.

To complement the photographic and videorecords, voucher specimens and samples for primary productivity experiments were collected. Specimens were taken along the lower to upper limits of living rhodolith distributions using a hydraulically operated, Petersen-type, manipulator grab sampler mounted on the submersible. All rhodoliths in $\approx$20 × 20-cm areas visually determined to be representative (typical) of a given depth range were harvested into separate numbered containers. Many of the nongeniculate coralline specimens proved to be unidentifiable to the species level due to a lack of reproductive structures and a high probability that most have not been taxonomically described, but at least seven genera were represented. Voucher materials were preserved in 5% formalin/seawater to be deposited in the algal collection of the US National Herbarium and the Harbor Branch Oceanographic Institution Herbarium.

PRIMARY PRODUCTIVITY

Samples of rhodoliths for productivity measurements were taken from two depths on the west side of the seamount [76 m (16–18 $\mu mol \cdot m^{-2} \cdot s^{-1}$ photosynthetically active

radiation) and 200 m (0.013–0.015 μmol $\cdot$ m^{-2} $\cdot$ s^{-1} PAR)] and kept at ambient temperature in darkness to prevent light shock. Care was taken to select individual rhodoliths that were similar in size and single species composition to those occurring within the transects assessed for cover.

In the cases of unidentified coralline algae, *Lithophyllum* sp., *Peyssonnelia* sp., and *Gypsina/Ostreobium* from the platform rhodoliths (76 m), incubations were done on four replicate fragments of living crusts at $\approx 1\%$ of the surface illumination (16–18 μmol $\cdot$ m^{-2} $\cdot$ s^{-1} PAR). A photosynthesis vs. irradiance (*PI*) curve was determined for the west slope whole-rhodolith samples from 200 m containing only the unidentified nongeniculate coralline. Incubations were conducted on shore in the dark and in direct sunlight that was reduced by multiple layers of neutral-density nylon window screening to obtain levels of photosynthetically active radiation (PAR = 0, 0.0002, 0.002, 0.01, and 0.1% of ambient sunlight) that were equivalent to those of the natural seamount habitats. The neutral density screening used to reduce intensity does so without preference to wavelength, unlike seawater (Jerlov Type I) which absorbs preferentially the red and UV ends of the spectrum. Dring (1981), Ramus & Van der Meer (1983), and Drew (1983) concluded that reduction in light quantity has the same effect on photosynthesis as increase in depth. Light was measured as (400–700 nm) and quality does not affect quantity when PAR is compared. In other words, PAR at depth was equal to the PAR used in our incubations.

Methods concerning the handling of algae, incubation, and O_2 analysis followed the recommendations of Littler (1979) and Littler & Arnold (1980), and were essentially similar to those employed by Littler et al. (1983). Four replicates from each of the various light levels were incubated individually in 1-l, wide-mouth, glass canning jars on the day following collection (30 October 1985) between 0900 and 1400 EST. Dark jars were wrapped with two layers of heavy-duty Al foil. The incubation bath was maintained at the temperature during collection (25 °C) by constant flushing. Whole rhodoliths were incubated in individual bottles that were continuously mixed with air-driven magnetic stirrers and Teflon-coated stir bars to disrupt any metabolically induced diffusion gradients. The water used was collected just prior to the experiments, filtered through a nannoplankton net (10 μm pore size), and vigorously poured between buckets to bring the O_2 level to ambient saturation.

Net productivity was measured to within 1 μg $O_2 \cdot l^{-1}$ with an Orbisphere 2610 O_2 analyser, and calculated as mg organic C fixed $\cdot$ g^{-1} of thallus organic dry weight (after chipping off the living thalli) or m^{-2} of 2-D thallus area (also determined by point intercept scoring) $\cdot$ h^{-1}, assuming a photosynthetic quotient of 1. As mentioned above, we measured planar area because of the close correlation of photosynthesis with 2-D area normal to the incoming radiation. The 2-D plant coverages $\cdot$ m^{-2} of substratum were multiplied by individual production rates $\cdot$ m^{-2} of planar thallus area to estimate the contribution of each rhodolith population to overall community production on the seamount (i.e., the slope and platform).

RADIOCARBON DATING

Radiocarbon dates were determined for 35 samples from 16 of the coralline-foraminiferan rhodoliths. Individual layers of coralline algae and the foraminiferan *Gypsina* could be analysed due to the small sample sizes measurable by accelerator mass spectrometry (AMS). The nodules were sectioned by water-lubricated diamond saw, and appropriate strata to be dated were identified under a dissection microscope. Samples were taken from the central cores, the transitional regions from the cores to the outer envelopes, and the relatively well-preserved subsurface crusts. ≈ 0.01 g of material was removed from each stratum by a Dremel grinder and placed in a labeled vial. In all cases, lithified and infilled material was avoided. 15 growth rates were calculated for the platform nodules by dividing the distance (mm) between dated layers by the age (ybp) of the innermost layer. Growth rates were not calculated for nodules from the slope, because well-defined internal layers generally were lacking and only central cores were aged.

Beta Analytic coordinated the radiocarbon analyses. The samples were given no pretreatment and reacted with phosphoric acid to produce CO_2, which was purified and then reacted with H on a Co catalyst to produce graphite. The graphite was applied to Cu targets. The AMS measurements were made in triplicate on aliquots of each milled sample at the Eidgenossische Technische Hochschule, University of Zürich.

RESULTS

RHODOLITH DISTRIBUTION AND ABUNDANCE

The platform surface of SSSM to a depth of 91 m is quite uniform and averages 95.8% cover of rhodoliths (Fig. 2A, Table I). This planar surface-area estimate is conservative as many regions contain at least five-deep (up to 45 cm) accumulations of rhodoliths (Fig. 3, Table II) with extensive living surfaces dominated by encrusting algae such as *Lithophyllum* sp. (41% mean cover), other nongeniculate corallines (14.9%), *Peyssonnelia* sp. (12.6%), and the foraminiferan *Gypsina* sp. (cf. *vesicularis*) (25%). Rhodolith cover on the seamount platform (95.8%) was much more uniform (i.e., relatively narrow confidence intervals, Table I) and significantly greater ($P < 0.05$, Bonferroni analysis) than that on the slopes (17.4%). The four platform transects did not differ significantly ($P > 0.05$, Bonferroni) in rhodolith cover, however the south transect on the seamount slope contained significantly less rhodolith cover ($P < 0.05$) than the other three slope transects (Table I). The overall rhodolith cover on the north slope transect was transitional in that it did not differ significantly ($P > 0.05$) from either the east or the west slope rhodolith coverages, which were significantly different from each other ($P < 0.05$, Bonferroni).

Examples of developing rhodoliths are numerous on the platform as evidenced by small-to-large (4–15 cm diameter) nodules containing a mixture of taxonomically problematical genera of nongeniculate coralline algae (e.g., *Neogoniolithon*, *Mesophyllum*,

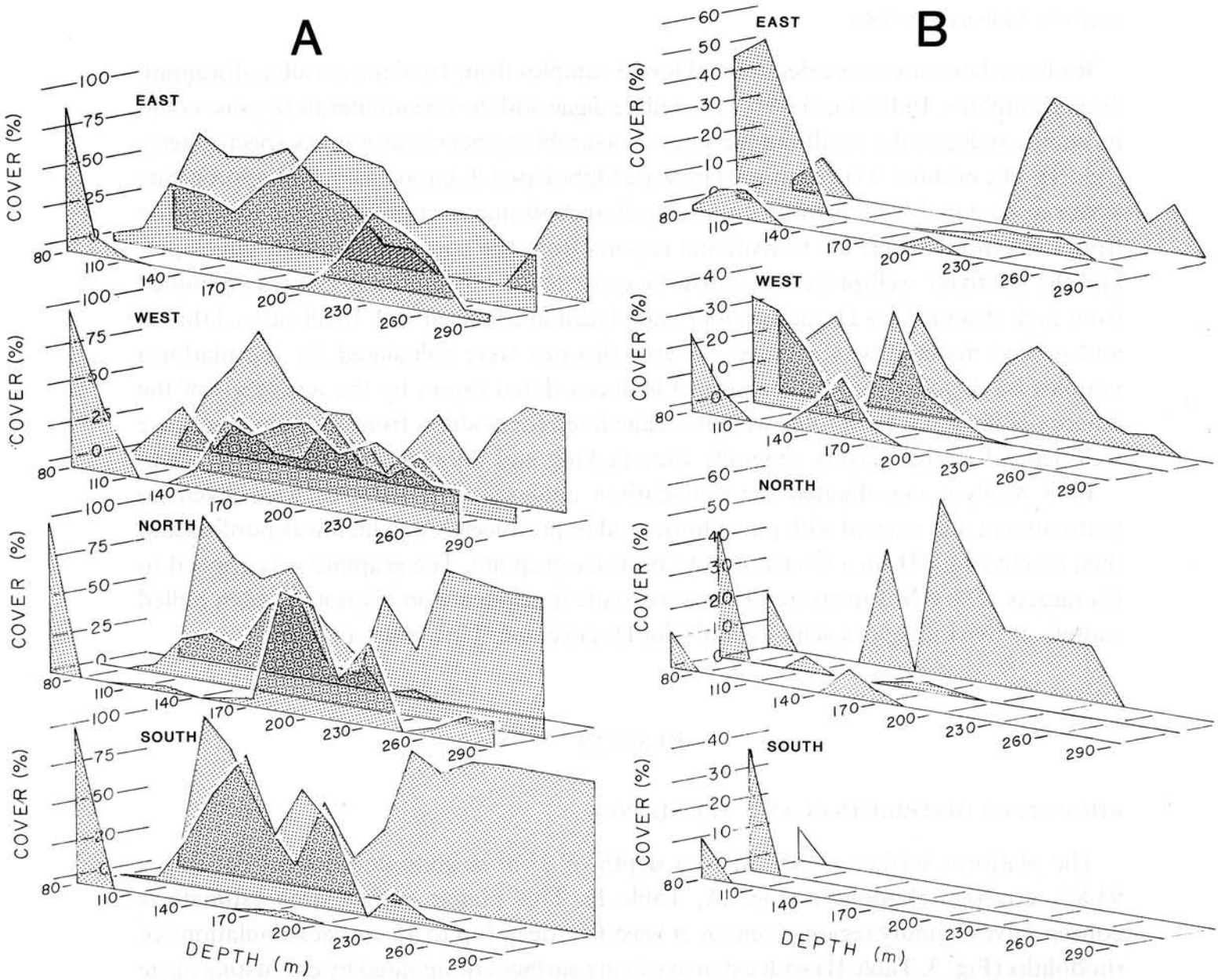

Fig. 2 (A) Distribution of substratum types [i.e., sand (front), bedrock (middle), and rhodoliths (rear)] in mean percent cover along four transects as a function of depth. (B) Distribution of living nongeniculate coralline algae (front), *Lithophyllum* sp. (middle), and *Peyssonnelia* sp. (rear) as mean percent cover on rhodoliths along four transects as a function of depth.

Lithophyllum, *Sporolithon*, *Titanoderma*, *Lithoporella*, and *Lithothamnion*), the squamariacean *Peyssonnelia*, *Gypsina* sp., and patches of small corals (e.g., *Madracis*, *Porites*, and *Leptoseris*; Fig. 4A), all being internally reworked by clionid sponges and other boring organisms. The rhodolith accumulations are overgrown by multilayered canopies of fleshy macroalgae (Fig. 3), forming a spatially complex community. *Lobophora variegata* (Lamour.) Womersley (59.4% mean cover) dominates the secondary canopy, while *Dictyota divaricata* Lamour. (8.9%), *Caulerpa peltata* Lamour. (5.5%), a large undescribed *Cladophora* sp. (0.1%), *Halimeda copiosa* Goreau & Graham (6.2%), *H. discoidea* Decaisne (4.5%), and an undescribed palmelloid green algae [cf. *Palmo-*

TABLE I

Mean distribution of percent cover for substratum types on four transects as a function of habitat and depth range. One-way ANOVA and a posteriori Bonferroni multiple classification results with significant differences at $P < 0.05$ indicated by *.

Habitat	Transect	Depth range (m)	Substratum cover (% ± SD)			N
			Sand	Bedrock	Rhodoliths	
Platform	East	77–91	4.3 ± 2.5	10.6 ± 12.8	85.2 ± 15.3	6
	West	77–91	0.8 ± 2.0	0.7 ± 1.6	98.5 ± 2.3	6
	North	67–76	0.0	0.5 ± 1.2	99.3 ± 1.2	6
	South	77–91	0.0	0.0	100.0 ± 0.0	6
$\bar{x}$			1.3	3.0	95.8	
Slope	East	92–290	53.4 ± 19.1	31.8 ± 25.2	15.0 ± 20.0	60
	West	92–290	24.5 ± 13.1	42.2 ± 22.4	33.3 ± 19.5	87
	North	92–290	50.6 ± 29.8	28.2 ± 34.9	21.2 ± 27.8	75
	South	92–290	27.7 ± 32.6	72.0 ± 32.8	0.3 ± 1.0	71
$\bar{x}$			39.0	43.6	17.4	

* Platform rhodolith cover > slope rhodolith cover
* Platform sand cover < slope sand cover
* Platform bedrock cover < slope bedrock cover
* South slope rhodolith cover < east, west, and north slope cover
* East slope rhodolith cover < west slope cover

TABLE II

Mean distribution of percent cover for living encrusting algae on rhodoliths on four transects as a function of habitat and depth. One-way ANOVA and a posteriori Bonferroni multiple classification results with significant differences at $P < 0.05$ indicated by *.

Habitat	Transect	Depth range (m)	Living encrusting algal cover (% ± SD)			N
			Nongeniculate corallines	*Lithophyllum* sp.	*Peyssonnelia* sp.	
Platform	East	77–91	3.4 ± 0.8	48.0 ± 6.4	3.0 ± 2.1	6
	West	77–91	18.2 ± 1.6	36.7 ± 16.4	26.3 ± 13.8	6
	North	67–76	16.9 ± 3.7	40.2 ± 11.0	11.3 ± 4.0	6
	South	77–91	21.0 ± 8.6	39.2 ± 10.2	10.0 ± 5.6	6
$\bar{x}$			14.9	41.0	12.6	
Slope	East	92–290	21.5 ± 15.7	12.8 ± 19.4	3.0 ± 4.4	27
	West	92–290	17.7 ± 10.2	10.2 ± 13.8	3.6 ± 6.0	71
	North	92–290	20.0 ± 20.0	1.0 ± 1.9	1.5 ± 3.5	37
	South	92–290	0.0	0.0	0.0	1
$\bar{x}$			14.8	6.0	2.0	

* Total platform cover > total slope cover
* *Lithophyllum* platform cover > *Lithophyllum* slope cover
* *Peyssonnelia* platform cover > *Peyssonnelia* slope cover

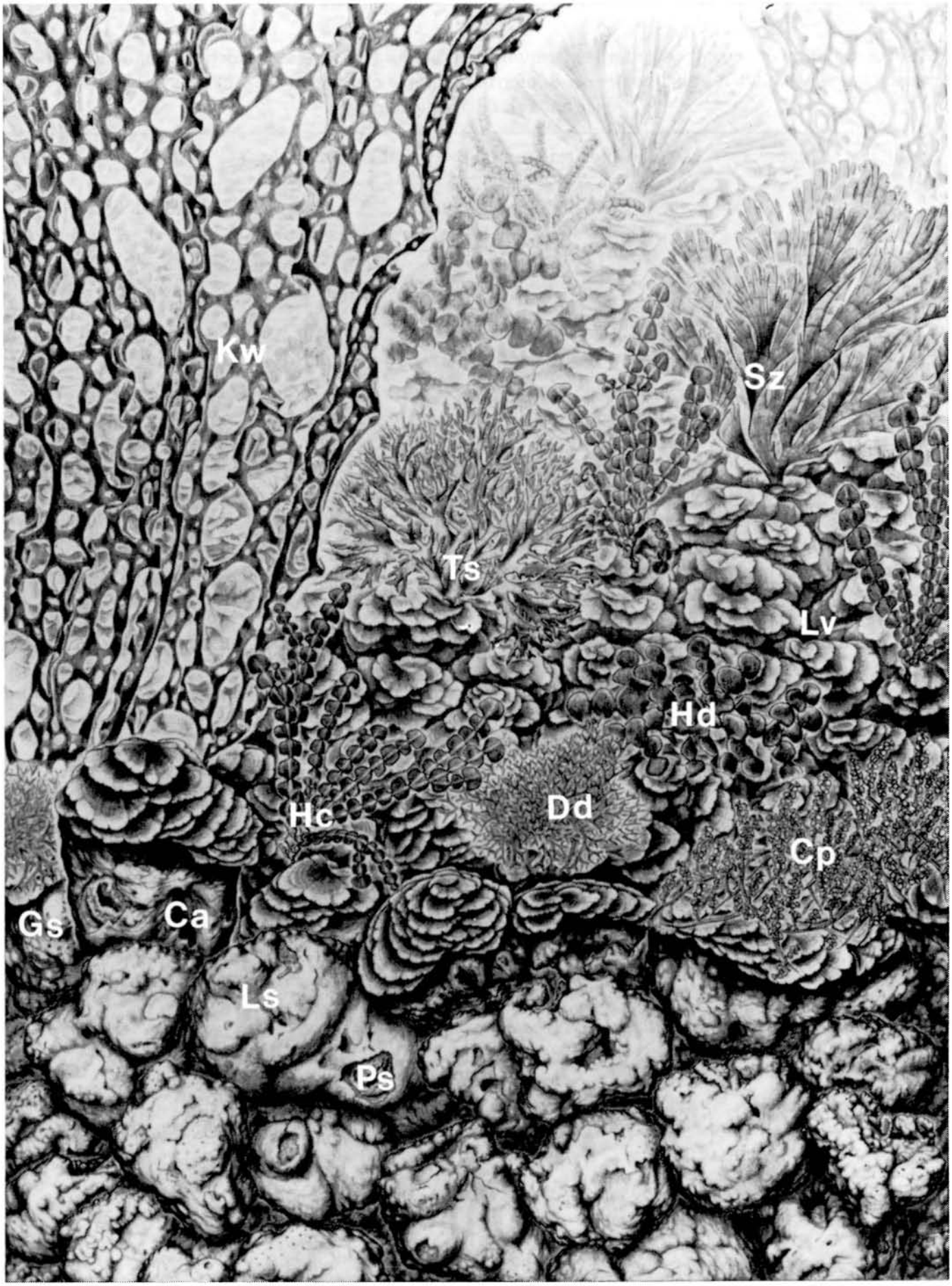

Fig. 3. Oblique sectional view of typical platform macroalgal dominated site of rhodolith formation drawn from videotaped recordings. Foreground shows primary substrata consisting of layered rhodoliths (each ≈9 cm in diameter) encrusted with nongeniculate coralline algae (Ca), *Gypsina* sp. (Gs), *Lithophyllum* sp.

TABLE III

Productivity (as C fixed ± SD, $N = 4$, at 1% of surface irradiance) and cover (%) of major contributors to rhodolith formation on seamount platform.

Taxa	Organic-based rates (mg C · g^{-1} · h^{-1})	Area-based rates (g C · m^{-2} thallus · h^{-1})	Cover on rhodoliths (%)	Rhodolith productivity (g C · m^{-2} total substratum · h^{-1})	Percent of total productivity
Nongeniculate corallines	0.43 ± 0.05	0.10 ± 0.01	14.9	0.015	17.0
Lithophyllum sp.	0.61 ± 0.07	0.14 ± 0.02	41.0	0.057	64.8
Peyssonnelia sp.	0.43 ± 0.11	0.06 ± 0.02	12.6	0.008	9.1
Gypsina/Ostreobium	0.39 ± 0.17	0.03 ± 0.01	25.0	0.008	9.1

phyllum crassum (Naccari) Rabenhorst] (0.4%) form a tertiary canopy. The uppermost canopy of large macroalgae (Fig. 3) includes *Kallymenia westii* Ganesan (4.6%), with occasional individual thalli of *Stypopodium zonale* (Lamour.) Papenfuss, *Sargassum hystrix* J. Ag., and an undescribed *Titanophora* sp. Large sponges, plate corals, gorgonians, and anemones are sparsely scattered throughout the platform community. Sand-sized and finer sediments are present but a minor component on the platform, being restricted to a layer beneath the predominant rhodoliths. Most silt-sized particles are evidently swept away by currents because only minor sand pockets were observed and sediments mainly occurred beneath the layered rhodoliths.

The slope of the seamount to 290 m averages 17.4% cover of rhodoliths (Table I) which clearly have spilled down to accumulate well below the shoulder of the platform (Fig. 4B), resembling terrestrial alluvial fans. These nodule fans are most prevalent on the west side (leeward) of the mount (33.3% cover) and are more abundant near the top of the west slope (Fig. 2A) than is the case on the other three sides. The east, north, and south transects (Fig. 2A) do not show rhodolith accumulations until below considerable depths. The north slope ranks second in rhodolith cover (22.4%) while the south side is virtually free of rhodoliths (0.3% cover) due to its current swept, steep, and relatively smooth slope (Table I). The windward east side of the mount (with a mean rhodolith cover of 15%) is nearly vertical to 200 m, so rhodoliths accumulate mainly below this depth (Fig. 2A).

Living calcareous algal cover of the slope rhodoliths averages only 22.8% and is made up of 14.8% nongeniculate corallines, 6% *Lithophyllum* sp., and 2% *Peyssonnelia* (Table II) which are not distributed in well-defined zones as a function of depth (Fig. 2B).

(Ls), and *Peyssonnelia* sp. (Ps). These are partly covered by a secondary canopy consisting of *Lobophora variegata* (Lv), which contains a tertiary canopy formed by *Caulerpa peltata* (Cp), *Dictyota divaricata* (Dd), *Halimeda copiosa* (Hc), and *Halimeda discoidea* (Hd). Tallest (fourth) canopy, shown to rear, consists of frondose algae, such as *Titanophora* sp. (Ts), *Stypopodium zonale* (Sz), and *Kallymenia westii* (Kw). This community of frondose algae on multiple layers of rhodoliths is widespread on platform (based on extensive grab-sample collections), except large brown alga *Sargassum hystrix* dominates fourth canopy level in patches towards eastern portion.

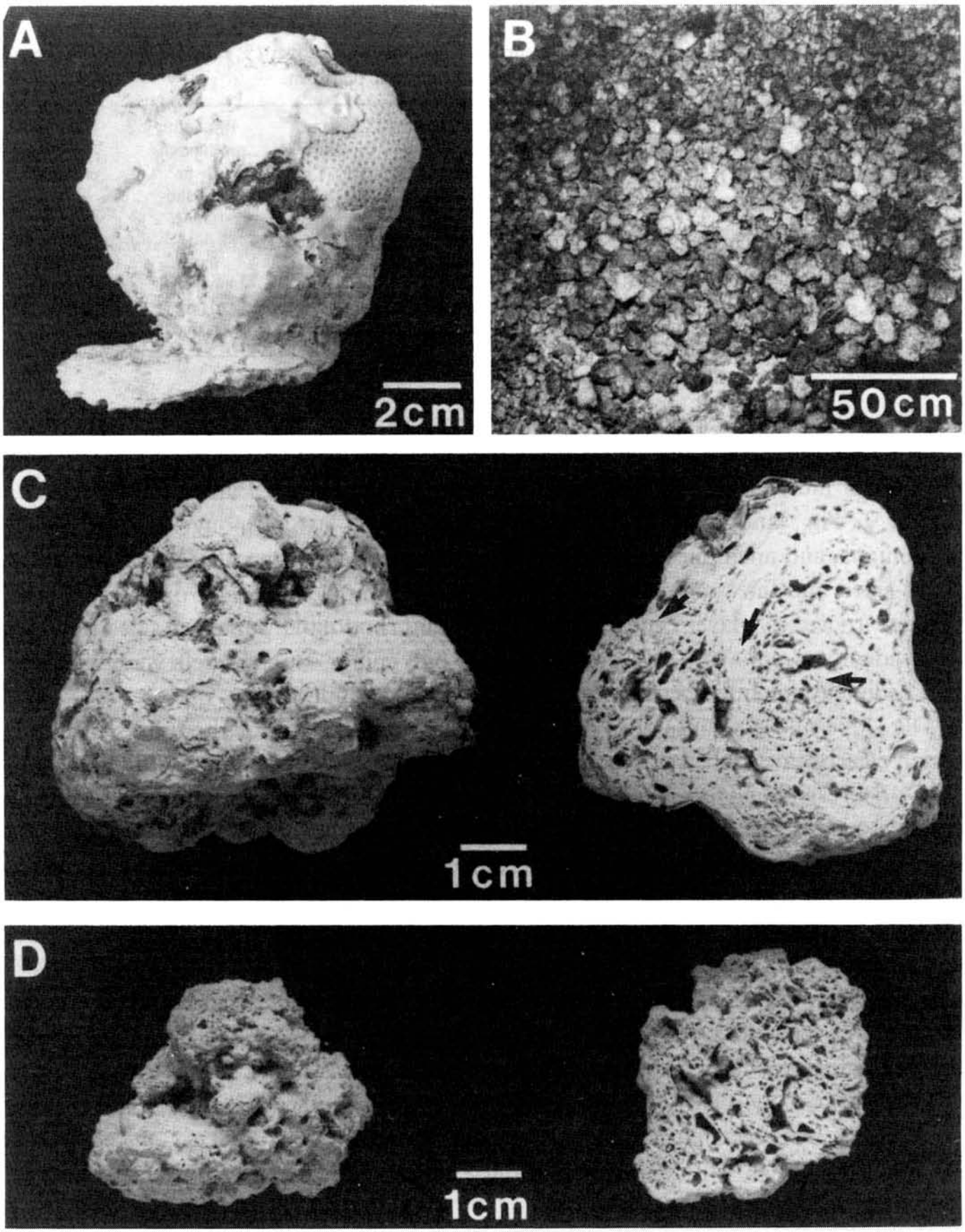

Fig. 4 (A) Rhodolith 6 (Table IV) that was secondarily cemented by a small coral plate of *Leptoseris cucullata* (Ellis & Solander) (bottom), broken off during collection from platform at 71 m. Coral on upper right is *Madracis pharensis* (Heller) ssp. *luciphila*, *Gypsina* sp. (cf. *vesicularis*) dominates upper central and left region, central dark area is *Peyssonnelia* sp., and lower basal area (*L. cucullata*) is covered by an unidentified nongeniculate coralline alga. (B) Characteristic rhodolith accumulations (west slope at a depth of 150 m). (C,D) Outer surfaces (left) and interior cross-sectional (right) views of representative rhodoliths. (C) Platform rhodolith (No. 5, Table IV) contains an outer smooth surface of *Gypsina* sp. and nongeniculate

Living encrusting algal coverage on the seamount slope rhodoliths was much more variable (Table II) than on the platform rhodoliths due to the extremely patchy nature of rhodolith accumulations on the slopes. Total encrusting algal coverage was significantly higher ($P < 0.05$, Bonferroni) on platform rhodoliths (68.5%) than on slope rhodoliths (22.8%) due to significantly greater coverages of both *Lithophyllum* sp. and *Peyssonnelia* sp. (Table II). *Gypsina* sp. and stony corals are not important components of slope nodules. The south slope transect shows no living rhodolith cover; the majority of rhodoliths containing live calcareous algae occur on the west slope (Fig. 2B). The east and north slope rhodoliths are characterized by reduced cover of *Lithophyllum* sp. and *Peyssonnelia* sp. The nodules spilling down the steep slopes of the seamount to depths of >200 m are characteristically smaller ($\bar{x} = \approx 5$ cm diameter, Fig. 4D), much rougher, and pitted by boring organisms. Consequently, they are more irregular in shape and contain reduced levels of living cover (Table II, Fig. 2B).

Biotic overstory on the seamount slopes becomes greatly diminished as a function of increasing depth below the platform and consists mostly of *Halimeda*, gorgonians, hydroids, and sponges along with scattered patches of small frondose algae, all of which occur primarily on the bedrock substratum. The eroded slope rhodoliths themselves do not support substantial cover of upright organisms.

RHODOLITH COMPOSITION

Rhodoliths do not vary greatly in composition over platform depths of 67–91 m (Fig. 2B) and mostly are 4–15 cm in diameter (Figs. 3,4C), with the majority being ≈9 cm. Our estimate of the mean crustose algal cover comprising the outer living envelopes of platform nodules (Table II) is 68.5%, composed of 41% *Lithophyllum* sp., 14.9% other nongeniculate corallines, 12.6% of the squamariacean alga *Peyssonnelia* sp., along with 25% cover of the crustose foraminiferan *Gypsina* sp. (cf. *vesicularis*). In most of the *Gypsina* sp. encrustations, a lower living layer of the rock-penetrating filamentous *Ostreobium* sp. gives the normally gray-brown *Gypsina* sp. a greenish-brown hue. Apparently, the tissues of *Gypsina* sp. contain photosymbionts (Prager & Ginsburg, 1989), as do the stony corals. *Gypsina* sp. competes vigorously with several species of nongeniculate coralline algae for space on the platform nodules. The dominant coralline algal crusts are bright red to maroon and can comprise up to 100% cover of the nodules. Only minor amounts of encrusting corals, such as *Madracis*, *Leptoseris*, and *Porites*, are present (Fig. 4A).

Cross sections through the centers of the platform rhodoliths (Fig. 4C) reveal outer, relatively thin (1–3 cm thick), living and well-preserved mantles overlying dead laminated crustose layers of mostly nongeniculate coralline algae and *Gypsina*

---

coralline algae while interior core is a combination of laminar and reworked coralline algae. Arrows indicate strata dated by AMS from left to right: internal edge of outer envelope, middle unaltered layer, and central altered core. (D) Slope rhodolith has a much rougher surface containing small patches of nongeniculate coralline algae and a large porous interior that is extensively bored, infilled, and lithified.

surrounding much thicker cores of altered carbonate. The nodules of the deeper seamount slopes (Fig. 4D) tend to lack an outer laminated envelope and, instead, are predominantly inner, reworked, carbonate core materials covered externally by variously sized crusts of coralline algae. In some deeper rhodoliths (Fig. 2B), small outer patches of *Peyssonnelia* cover are also important. The internal core materials of virtually all rhodoliths collected (Fig. 4C,D) have been extensively altered and reworked by boring sponges, algae, polychaetes, and pelecypods. Burrows have been infilled with carbonate detritus and lithified to various degrees ranging from porous to dense and stony.

PRIMARY PRODUCTIVITY

Rhodolith productivity on the 1.27-km^2 seamount platform is conservatively estimated to be $\approx$391 t organic C $\cdot$ yr^{-1} based on: (1) 95.8% visible planar cover of rhodoliths (Table I); (2) a mean production rate of 0.088 g C $\cdot$ m^{-2} $\cdot$ h^{-1} (summed from the fourth column of Table III); and (3) assuming a sustained 10 h $\cdot$ day^{-1} production at this rate. The productivity rates of the four major contributors to rhodolith formation on the platform habitat are given in Table III. *Lithophyllum* sp. is the highest producer at 0.14 g C $\cdot$ m^{-2} thallus $\cdot$ h^{-1} (0.61 mg C $\cdot$ g^{-1} organic dry wt $\cdot$ h^{-1}) and contributes nearly two-thirds of the rhodolith-former productivity of the platform community. The *Gypsina–Ostreobium* association contributes a surprisingly high 9.1% (Table III), although the latter is the lowest individual producer of the predominant rhodolith formers (0.03 g C $\cdot$ m^{-2} thallus $\cdot$ h^{-1}). Nongeniculate coralline algae and *Peyssonnelia* sp. contribute 17 and 9.1%, respectively, to the total primary productivity of platform rhodoliths.

Our time and resources permitted only one *PI* curve (Fig. 5) for one dominant crustose algal species from the slope nodules. This unidentified nongeniculate coralline occurs to 268 m (Littler et al., 1985) and reaches its photosynthetic peak of 0.012 mg

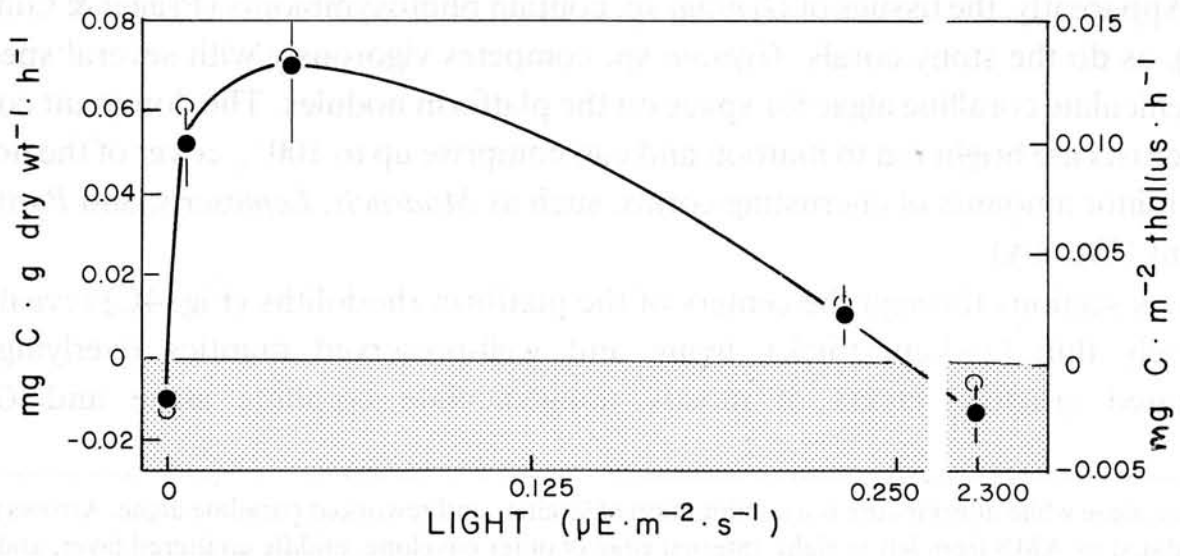

Fig. 5. *PI* response of dominant nongeniculate coralline from slope (200 m). Solid circles are values for g organic dry thallus wt ($\pm$ SD, N = 4), open circles are for m^2 algal thallus.

$C \cdot m^{-2}$ thallus $\cdot h^{-1}$ (0.07 mg C $\cdot$ g organic dry $wt^{-1} \cdot h^{-1}$) at 0.002% of the maximum surface irradiance (0.05 μmol $\cdot m^{-2} \cdot s^{-1}$ PAR). It shows positive net photosynthesis over the extremely narrow light range from somewhat beyond 0.24–0.005 μmol $\cdot m^{-2} \cdot s^{-1}$. This light range is equivalent to the depth interval from $\approx$100 to 220 m with P_{max} occurring at 135 m. Dark respiration is $\approx$17% of the maximum net photosynthetic rate (Fig. 5). By taking the mean net photosynthetic rate data (0.008 g $C \cdot m^{-2}$ thallus $\cdot h^{-1}$) and mean nongeniculate coralline cover on rhodoliths (22.8%, Table II) over the above depth range, we estimate a net contribution to slope rhodolith productivity of 0.002 mg $C \cdot m^{-2}$ rhodoliths $\cdot h^{-1}$ by this alga.

TABLE IV

Radiocarbon dates (ybp $\pm$ SD, $N = 3$) for outer, middle subsurface, and biotically altered center portions of platform and slope rhodoliths. Parentheses indicate growth rates in mm $\cdot yr^{-1}$ calculated from distances and ages between inner and outer layers.

Location, depth and sample	Portion of rhodolith		
	Internal portions of outer envelopes	Middle subsurface unaltered layers	Center altered cores
Platform (70 m)			
1	114 ± 9 (0.04)	200 ± 75 (0.04)	625 ± 70 (0.05)
2	215 ± 100 (0.02)	1100 ± 105 (0.04)	1295 ± 115 (0.03)
3	635 ± 100 (<0.01)	–	1195 ± 110 (0.04)
4	600 ± 95	995 ± 100 (0.01)	910 ± 95 (0.03)
5	450 ± 100 (0.01)	850 ± 100 (0.04)	1030 ± 100 (0.05)
6	112 ± 0.7 (0.02)	510 ± 60 (0.04)	825 ± 60 (0.04)
10	880 ± 105 (0.01)	–	1285 ± 110 (0.02)
$\bar{x}$	429 (0.02)	731 (0.03)	1023 (0.04)
Slope (219 m)			
7	1530 ± 105	–	1410 ± 100
8	980 ± 75	–	2070 ± 110
11	1610 ± 115	–	1925 ± 110
12	–	–	1360 ± 70
13	755 ± 70	–	1265 ± 70
14	770 ± 80	–	1270 ± 110
15	790 ± 75	–	1160 ± 70
16	1580 ± 80	–	–
$\bar{x}$	1145	–	1494
Slope (297 m)			
9	2385 ± 105	–	2480 ± 120

RADIOCARBON DATES

Radiocarbon dates were obtained for 35 samples from 16 representative rhodoliths (Table IV). By using AMS to analyse small tissue samples, it was possible to age the individual layers of algal and foraminiferan crusts made accessible by sectioning the nodules. We were particularly interested in dating the outermost subsurface intact layers, innermost unaltered crusts adjacent to core material, and the central cores (Fig. 4C). Coralline algae and *Gypsina* from surface crusts gave contemporary dates as expected, while dates from the biologically altered centers of platform nodules averaged 1023 ybp (range = 625–1295 ybp). The innermost unaltered layers averaged 731 ybp (range = 200–1100 ybp), while the predominant coralline algal layers from the outermost regions (mostly corallines) that were relatively unaltered by borers yielded radiocarbon dates averaging 429 ybp (range = 112–880 ybp). On the slopes, the outermost unaltered regions of nodules averaged much older ($\bar{x}$ = 1145 ybp, range = 755–1610 ybp) than those of the platform, as was the case for the altered central cores ($\bar{x}$ = 1494 ybp, range = 1160–2070 ybp).

The calculated growth rates for the platform nodules ranged from <0.01 to 0.05 mm $\cdot$ yr^{-1} (Table IV). Growth rates from central core areas to the middle layers averaged 0.04 mm $\cdot$ yr^{-1}, rates from the middle layers to the unaltered internal portions of the outer envelopes averaged 0.03 mm $\cdot$ yr^{-1}, whereas the most recent growth declined to only 0.02 mm $\cdot$ yr^{-1}.

DISCUSSION

This study provides the first quantitative measures of deep-water rhodolith distribution and abundance at sites of both active formation and subsequent breakdown. The west and north slopes of the seamount contain the largest populations of rhodoliths (33.9 and 21.2% cover, respectively) that clearly have spilled downward from the platform presumably due to infrequent hurricanes or severe tropical storms. The inherent instability of this dynamic process probably explains the shallower distributions, lack of well-defined zones, and the reduction of slope overstory species compared to those recorded (Littler et al., 1986) for the more stable, predominantly bedrock, substratum of the south slope of SSSM. Although we found living crustose algal cover on rhodoliths as deep as 290 m, active growth of rhodoliths occurred mainly at depths of <91 m (the lowest portion of the platform) as indicated by the thick, living and dead, structurally intact, outer layers. Similarly, an abundance of *Neogoniolithon* rhodoliths has been described (Blanc, 1968) for current-swept submarine plateaus in the Mediterranean at depths of 80–90 m. Rhodoliths form extensive areas of maerl that extend to slope depths of 60 m in the Mediterranean (Jacquotte, 1962; Peres, 1967; Caulet, 1972). Active growth of foraminiferan–algal nodules on shelf slopes in the eastern Caribbean and Florida (Reid & Macintyre, 1988; Prager & Ginsburg, 1989) appears to be limited to depths of 30–60 m. On Hawaiian reef slopes, living rhodoliths are abundant between

depths of 60–90 m (Adey et al., 1982). The greatest depth for algal growth on nodules in the Canary Islands was found (McMaster & Conover, 1966) to be 60–70 m, although spherical coralline nodules occur lined up in sand troughs to 100 m.

Many investigators have sought to explain the spherical morphology of deep-water rhodoliths, generally invoking some hydrological or biological mechanism for frequent turning. Recently, Prager & Ginsburg (1989) suggested, from in situ observations (35–65 m deep), that only infrequent slight repositioning is required to balance growth because the only surfaces restricted from active encrustation are those directly contacting sediments. Alternative testable hypotheses that might account for the characteristic spheroidal morphology of deep-water rhodoliths are that (1) metabolite translocation from upper to lower surfaces, or (2) heterotrophic utilization of dissolved organic energy sources could account for balanced envelope growth under uneven illumination. It is unlikely that currents or storms frequently tumble the 45-cm thick strata of rhodoliths on the platform of SSSM because currents of such magnitude would eliminate the delicate perennial frondose algae that predominate (Fig. 3) and export most or all of the rhodoliths to the slopes. Catastrophic events of such large magnitude (e.g., severe tropical storms or hurricanes) may have occurred in the distant past, accounting for the much greater ages of the slope nodules compared to those now on the platform (Table IV). In agreement with the observations of Reid & Macintyre (1988) on foraminiferan–algal nodules in the eastern Caribbean, once the rhodoliths have begun to cascade downslope they tend to lack complete envelopes, with only patches of living layers, and are relatively eroded and irregularly shaped compared to those of the platform. This pattern becomes more pronounced as a function of depth.

The present study also provides the first estimates of the contribution of rhodoliths to deep-sea productivity, with the unexpected finding of a severely restricted *PI* curve of net primary production (range = $\approx \pm 0.24\ \mu\text{mol} \cdot \text{m}^{-2} \cdot \text{s}^{-1}$ PAR; Fig. 5) for the species of nongeniculate coralline measured. This observation suggests that some individual deep-water benthic algae may be acclimated to extremely narrow light ranges, reflective of their consistent light environments. Maximum photosynthesis occurred at a light level equivalent to the maximum attained at ≈ 135 m, although the material incubated came from 200 m.

In comparison to other deep-water functional-form groups of algae, the crusts that form rhodoliths are among the lowest primary producers measured to date. For example, the organic-based photosynthetic rates ranged from 0.39 to 0.61 mg $\text{C} \cdot \text{g}^{-1} \cdot \text{h}^{-1}$ for rhodolith formers (Table III) vs. rates as high as 7.12 mg $\text{C} \cdot \text{g}^{-1} \cdot \text{h}^{-1}$ for deep-water frondose macroalgae (Littler et al., 1986). However, because these crusts are so abundant on rhodoliths, their contribution to rhodolith productivity $\cdot \text{m}^{-2}$ (range = 0.008–0.057 g $\text{C} \cdot \text{m}^{-1} \cdot \text{h}^{-1}$) can exceed that of other deep-water algae [range = < 0.001–0.035 g $\text{C} \cdot \text{m}^{-2}$ of bedrock $\cdot \text{h}^{-1}$; Littler et al. (1986)]. The higher productivity of *Lithophyllum* sp. (0.14 g $\text{C} \cdot \text{m}^{-2}$ thallus $\cdot \text{h}^{-1}$), in conjunction with its relatively greater cover (41%) on rhodoliths, make it the major contributor (64.8%) to rhodolith primary production on the seamount platform. The animal–plant association

Gypsina–Ostreobium, while by far the lowest producer of all nodule formers, because of its large cover contributes an average of 9.1% of the total platform rhodolith primary productivity. The contribution of crustose algae on rhodoliths to the total productivity of the seamount platform (0.088 g $C \cdot m^{-2} \cdot h^{-1}$) exceeds that of all fleshy and upright algae combined (0.053 g $C \cdot m^{-2} \cdot h^{-1}$; Littler et al., 1986).

The rhodoliths from SSSM did not contain measurable cover of shallow-water species of nongeniculate coralline algae which are often branched or contain knobby protuberances. Other workers (i.e., Reid & Macintyre, 1988) have noted an abundance of such shallow taxa [e.g., *Hydrolithon boergesenii* (Fosl.) Fosl., *Neogoniolithon mammilare* (Harvey) Setch. & Mason, *Lythophyllum congestum* (Fosl.) Fosl.] on island shelf nodules dredged between 60 and 90 m and, consequently, cautioned against using fossil nodules as paleoenvironmental indicators of depth. Even the shallowest rhodoliths (67 m) from the highest north-western portion of SSSM were not composed of the easily recognized shallow-water nongeniculate coralline algae. The isolation by deep waters of SSSM from shallow sources of rhodoliths may be responsible.

Radiocarbon dates for platform nodules indicate that the outermost unaltered envelopes underlying actively growing crusts are 112–880 yr old, with growth rates averaging < 0.01–0.04 mm $\cdot$ yr^{-1} ($\bar{x} = 0.02$). Growth rates were higher (nearly double) in the older portions of these same rhodoliths, indicating either a deterioration in conditions favoring rapid development or a decline in accretion rates as a function of age and size. Perhaps the colonization by epiphytic overstory communities in the not-so-distant past has slowed the growth of calcareous rhodolith formers on the platform. At the depths of SSSM, coralline algal growth rates would be predictably slow and this is substantiated by the inordinately low photosynthetic rates we obtained. It has been estimated (Adey & Macintyre, 1973) that continuously growing deep-water rhodoliths 30 cm in diameter could be as old as 800 yr, indicating very low growth rates. The core nuclei of both the platform and slope rhodoliths on SSSM vary in age, but they are all modern and not relict deposits formed during times of lower sea levels.

Our range of dates for unaltered envelopes (112–880 ybp) is not substantially different from the dates previously reported (330–645 ybp) for diverse regions (McMaster & Conover, 1966; Focke & Gebelein, 1978; Reid & Macintyre, 1988). The point is that nodules from all regions show discontinuities in growth. However, rather than indicating the single hiatus posited by Reid & Macintyre (1988), the dates are different at different places and even within a single place (in the case of SSSM). The question then becomes, why were there discontinuities (at one time or another)? We suggest the most parsimonious answer can be derived from our first-hand observations of multiple-layered, 45-cm thick accumulations of rhodoliths on SSSM platform and the equally thick nodule fans that have cascaded down the slopes (Figs. 3,4B), in conjunction with our relatively large sample sizes of radiocarbon dates (Table IV). The uppermost layers of nodules show the greatest enveloping living cover and thicker intact crusts relative to the buried nodules. The latter tend to decrease in living cover (particularly plant cover), becoming dormant and dead (indicated by bleaching) as a function

of depth of burial. Such observations imply cessation of active growth due to burial whereupon bioerosive organisms rework core materials, followed by later re-exposure to light and recolonization by encrusting coralline algae and *Gypsina*. Therefore, it seems highly probable that at some point in their long histories, most rhodoliths are likely to become buried and the lengths of burial can vary from several hundred to many hundreds of years, which will be reflected as discontinuities in their growth patterns.

Acknowledgements

We thank D.T. Gerace for his hospitality at the College Center of the Finger Lakes Bahamian Field Station. Appreciation is extended to J.A. Kilar and G.M. Burzycki for field assistance and to B.L. Brooks and S.A. Reed for laboratory work. I.G. Macintyre and R.P. Reid provided helpful discussion and comments on the manuscript. S.D. Cairns kindly identified the coral samples. The artwork used in Fig. 2 was provided by C. Feller; J. Piraino and T.A. Smoyer assisted with production of the photographic plates. This study would not have been possible without the combined skills and professionalism of the R/V *JOHNSON* ship crew and the *JOHNSON-SEA-LINK I* submersible crew.

References

Adey, W.H. & I.G. Macintyre, 1973. Crustose coralline algae: a re-evaluation in the geological sciences. *Bull. Geol. Soc. Am.*, Vol. 84, pp. 883–903.

Adey, W.H., R.A. Townsend & W.T. Boykins, 1982. The crustose coralline algae (Rhodophyta: Corallinaceae) of the Hawaiian Islands. *Smithson. Contrib. Mar. Sci.*, Vol. 15, pp. 1–74.

Barnes, J., D.J. Bellamy, D.J. Jones, B.A. Whitton, E.A. Drew, L. Kenyon, J.N. Lythoge & B.R. Rosen, 1971. Morphology and ecology of the reef front of Aldabra. *Symp. Zool. Soc. London*, Vol. 28, pp. 87–114.

Blanc, J.J., 1968. The sediments of the Mediterranean Sea. *Annu. Rev. Oceanogr. Mar. Biol.*, Vol. 6, pp. 373–454.

Bosellini, A. & R.N. Ginsburg, 1971. Form and internal structure of recent algal nodules (Rhodolites) from Bermuda. *J. Geol.*, Vol. 79, pp. 669–682.

Bosence, D.W.J., 1983. The occurrence and ecology of recent rhodoliths — a review. In, *Coated grains*, edited by T. Peryt, Springer, Berlin, pp. 225–242.

Caulet, J.P., 1972. Recent biogenic calcareous sedimentation on the Algerian shelf. In, *The Mediterranean Sea*, edited by D.J. Stanley, Dowden Hutchinson and Ross, Stroudsburg, Pennsylvania, pp. 261–278.

Drew, E.A., 1983. Light, In, *Sublittoral ecology: the ecology of the shallow sublittoral benthos*, edited by R. Earll & D.G. Erwin, Clarendon Press, Oxford, pp. 10–57.

Dring, M.J., 1981. Chromatic adaptation of photosynthesis in benthic marine algae: an examination of its ecological significance using a theoretical model. *Limnol. Oceanogr.*, Vol. 26, pp. 271–284.

Earle, S.A., 1985. Equipment for conducting research in deep waters. In, *Handbook of phycological methods. Ecological field methods: macroalgae*, edited by M.M. Littler & D.S. Littler, Cambridge University Press, Cambridge, pp. 233–252.

Faure, G. & L. Montaggioni, 1976. Les récifs coralliens Au-Vent de l'île Maurice (archipel des Mascareignes, Océan indien): géomorphologie et bionomie de la pente externe. *Mar. Geol.*, Vol. 21, pp. M9–M16.

Focke, J.W. & C.D. Gebelein, 1978. Marine lithification of reef rock and rhodoliths at a fore-reef slope locality (−50 m) off Bermuda. *Geol. Mijnbouw*, Vol. 57, pp. 163–171.

Hay, M.E., 1986. Functional geometry of seaweeds: ecological consequences of thallus layering and shape

in contrasting light environments. In, *On the economy of plant form and function*, edited by T.J. Givnish, Cambridge University Press, Cambridge, pp. 635–666.

Jacquotte, P., 1962. Etude des fonds de maerl de la Méditerranée. *Rec. Trav. Stn. Mar. Endoume Marseille*, Vol. 26, pp. 141–235.

Jerlov, N.G., 1970. Light. In, *Marine ecology. Vol. 1. Environmental factors*, edited by O. Kinne, Wiley-Interscience, London, pp. 95–102.

Littler, M.M., 1973. The distribution, abundance and communities of deep-water Hawaiian crustose corallines (Rhodophyta, Cryptonemiales). *Pac. Sci.*, Vol. 27, pp. 281–289.

Littler, M.M., 1979. The effects of bottle volume, thallus weight, oxygen saturation levels, and water movement on apparent photosynthetic rates in marine algae. *Aquat. Bot.*, Vol. 7, pp. 21–34.

Littler, M.M. & K.E. Arnold, 1980. Sources of variability in macroalgal primary productivity: sampling and interpretative problems. *Aquat. Bot.*, Vol. 8, pp. 141–156.

Littler, M.M. & D.S. Littler, 1985. Non-destructive sampling. In, *Handbook of phycological methods. Ecological field methods: macroalgae*, edited by M.M. Littler & D.S. Littler, Cambridge University Press, Cambridge, pp. 161–175.

Littler, M.M., D.S. Littler, S.M. Blair & J.N. Norris, 1985. Deepest known plant life discovered on an uncharted seamount. *Science*, Vol. 227, pp. 57–59.

Littler, M.M., D.S. Littler, S.M. Blair & J.N. Norris, 1986. Deep-water plant communities from an uncharted seamount off San Salvador Island, Bahamas: distribution, abundance, and primary productivity. *Deep Sea Res.*, Vol. 33, pp. 881–892.

Littler, M.M., D.S. Littler & P.R. Taylor, 1983. Evolutionary strategies in a tropical barrier reef system: functional-form groups of marine macroalgae. *J. Phycol.*, Vol. 19, pp. 229–237.

Logan, B.W., J.L. Harding, M. Ahr, J.D. Williams & R.G. Sleep, 1969. Late Quaternary carbonate sediments of the Yucatan Shelf, Mexico. *Mem. Am. Assoc. Petrol. Geol.*, Vol. 11, pp. 5–128.

McMaster, R.L. & J.T. Conover, 1966. Recent algal stromatolites from the Canary Islands. *J. Geol.*, Vol. 74, pp. 647–652.

Minoura, K. & T. Nakamori, 1982. Depositional environment of algal balls in the Ryukyu Group, Ryukyu Islands, southwestern Japan. *J. Geol.*, Vol. 90, pp. 602–609.

Peres, J., 1967. The Mediterranean benthos. *Annu. Rev. Oceanogr. Mar. Biol.*, Vol. 5, pp. 449–533.

Prager, E.J. & R.N. Ginsburg, 1989. Carbonate nodule growth on Florida's outer shelf and its implications for fossil interpretations. *Palaios*, Vol. 4, pp. 310–317.

Ramus, J. & J.P. Van der Meer, 1983. A physiological test of the theory of complementary chromatic adaptation. I. Color mutants of a red seaweed. *J. Phycol.*, Vol. 19, pp. 86–91.

Reid, R.P. & I.G. Macintyre, 1988. Foraminiferal-algal nodules from the eastern Caribbean: growth history and implications on the value of nodules as paleoenvironmental indicators. *Palaios*, Vol. 3, pp. 424–435.

SAS, 1985. *SAS user's guide: basics*. SAS Institute, Cary, North Carolina.

Scoffin, T.P., D.R. Stoddart, A.W. Tudhope & C. Woodroffe, 1985. Rhodoliths and coralliths of Muri Lagoon, Rarotonga, Cook Islands. *Coral Reefs*, Vol. 4, pp. 71–80.

Sokal, R.R. & F.J. Rohlf, 1969. *Biometry*. Freeman, San Francisco, 776 pp.

Toomey, D.C., 1975. Rhodoliths from the Upper Paleozoic of Kansas and the Recent – a comparison. *Neues Jahrb. Geol. Paläontol. Monatsh.*, Vol. 4, pp. 242–255.

Weber-van Bosse, A. & M. Foslie, 1904. The Corallinaceae of the Siboga Expedition. *Siboga Exped.*, Vol. 61, pp. 1–110.

Weydert, P., 1974. Morphologie et sédimentologie de la pente externe de la partie nord du Grand Réarcif de Tuléar (SW de Madagascar): nature et répartition des éléments organogènes libres. *Mar. Geol.*, Vol. 17, pp. 299–337.